

# Survivin modulates stiffness-induced vascular smooth muscle cell motility

Cite as: APL Bioeng. 9, 026120 (2025); doi: 10.1063/5.0252766

Submitted: 11 December 2024 · Accepted: 6 May 2025 ·

Published Online: 4 June 2025



View Online



Export Citation



CrossMark

Thomas Mousso,<sup>1</sup>  Kalina Rice,<sup>1</sup> Bat-Ider Tumenbayar,<sup>2</sup> Khanh Pham,<sup>1</sup>  Yuna Heo,<sup>1,3</sup>  Su Chin Heo,<sup>3</sup>   
Kwonmoo Lee,<sup>4</sup>  Andrew T. Lombardo,<sup>5</sup>  and Yongho Bae<sup>1,6,a)</sup> 

## AFFILIATIONS

<sup>1</sup>Department of Pathology and Anatomical Sciences, Jacobs School of Medicine and Biomedical Sciences, University at Buffalo, Buffalo, New York 14203, USA

<sup>2</sup>Department of Pharmacology and Toxicology, Jacobs School of Medicine and Biomedical Sciences, University at Buffalo, Buffalo, New York 14203, USA

<sup>3</sup>Department of Orthopedic Surgery, Perelman School of Medicine, University of Pennsylvania, Philadelphia, Pennsylvania 19104, USA

<sup>4</sup>Vascular Biology Program, Boston Children's Hospital, Boston, Massachusetts 02115, USA

<sup>5</sup>Department of Biochemistry, Jacobs School of Medicine and Biomedical Sciences, University at Buffalo, Buffalo, New York 14203, USA

<sup>6</sup>Department of Biomedical Engineering, School of Engineering and Applied Sciences, University at Buffalo, Buffalo, New York 14260, USA

**Note:** This paper is part of the Special Topic on Mechanomedicine.

<sup>a)</sup> Author to whom correspondence should be addressed: [yonghoba@buffalo.edu](mailto:yonghoba@buffalo.edu)

## ABSTRACT

Arterial stiffness is a contributor to cardiovascular diseases (CVDs) and is associated with the aberrant migration of vascular smooth muscle cells (VSMCs). However, the mechanisms driving VSMC migration in stiff environments remain unclear. We recently demonstrated that survivin is upregulated in mouse and human VSMCs cultured on stiff hydrogels, where it modulates stiffness-mediated cell proliferation. However, its role in stiffness-dependent VSMC migration remains unknown. To assess its impact on migration, we performed time-lapse microscopy on VSMCs seeded on fibronectin-coated soft and stiff hydrogels, mimicking the physiological stiffness of normal and diseased arteries. We observed that VSMC motility increased under stiff conditions, while pharmacologic or siRNA-mediated inhibition of survivin reduced stiffness-stimulated migration to rates similar to those observed under soft conditions. Further investigation revealed that cells on stiff hydrogels exhibited greater directional movement and robust lamellipodial protrusion compared to those on soft hydrogels. Interestingly, survivin-inhibited cells on stiff hydrogels showed reduced directional persistence and lamellipodial protrusion. We also found that survivin overexpression modestly increased cell motility and partially rescued the lack of directional persistence compared to green fluorescent protein (GFP)-expressing VSMCs on soft hydrogels. Mechanistically, stiffness- and survivin-dependent cell migration involves focal adhesion kinase (FAK) and actin dynamics, as stiffness increases phosphorylated FAK recruitment to focal adhesions and promotes actin organization and stress fiber formation—effects that are disrupted by survivin inhibition. In conclusion, our findings establish that mechanotransduction through a survivin–FAK–actin cascade converts extracellular matrix stiffness into stiffness-sensitive motility, suggesting that targeting this pathway may offer therapeutic strategies for CVD.

© 2025 Author(s). All article content, except where otherwise noted, is licensed under a Creative Commons Attribution-NonCommercial-NoDerivs 4.0 International (CC BY-NC-ND) license (<https://creativecommons.org/licenses/by-nc-nd/4.0/>). <https://doi.org/10.1063/5.0252766>

## I. INTRODUCTION

Arterial stiffness accelerates the progression of various cardiovascular diseases (CVDs) and pathologies, including atherosclerosis, stroke, hypertension, and neointimal hyperplasia.<sup>1–4</sup> Within the tunica media of the vessel, vascular smooth muscle cells (VSMCs) sense

increased matrix stiffness caused by vascular injury or elevated high blood pressure, undergoing a phenotypic transition from a contractile to a synthetic state. This shift is characterized by abnormal proliferation, increased synthesis of extracellular matrix (ECM) proteins, and aberrant migration toward the tunica intima,<sup>5,6</sup> contributing to

neointima formation. While reducing arterial stiffness mitigates atherosclerosis<sup>7</sup> and neointimal hyperplasia,<sup>2</sup> the underlying mechanisms responsible for the abnormal cellular behavior observed in stiffened regions remain unclear. Various CVD medications, including lipid-lowering agents, antiplatelet drugs, and antihypertensive drugs,<sup>8</sup> have been shown to reduce atherosclerotic plaque formation; however, no current therapy specifically targets arterial stiffening or the associated abnormal cellular behaviors. In addition, drug-eluting stents, which reduce restenosis when combined with antiproliferative and antimigratory agents,<sup>9</sup> can increase the risk of thrombosis by delaying the reendothelialization process.<sup>10–12</sup> Therefore, a deeper understanding of the molecular mechanisms through which arterial stiffness contributes to the progression of various CVDs through modulation of VSMC behaviors may lead to a novel therapeutic strategy.

Survivin, also known as Baculoviral IAP Repeat Containing 5 (Birc 5), belongs to the inhibitors of apoptosis (IAPs) protein family. Survivin has been predominately studied in the context of cancer, where it regulates apoptosis, proliferation, and migration.<sup>13–16</sup> In cardiovascular biology, limited studies have identified its role in the progression of neointimal hyperplasia, heart failure, atherosclerosis, and pulmonary arterial hypertension.<sup>17–22</sup> Adenoviral delivery of a functionally defective survivin mutant attenuated neointimal hyperplasia in mouse<sup>23</sup> and rabbit<sup>17</sup> vascular injury models, implying its direct role in this process. Furthermore, given the critical role of stiffness in CVDs, we recently observed significantly elevated survivin expression on high pathological stiffness matrices compared to soft, physiological stiffness in mouse and human VSMCs using an *in vitro* stiffness-tunable polyacrylamide hydrogel model.<sup>24,25</sup> We further found that survivin plays an important role in regulating cell cycle progression, proliferation, intracellular stiffness, and ECM synthesis under stiff conditions—key cellular processes that drive the progression of CVDs. Aberrant cell migration is another crucial component in promoting various CVDs and pathologies. Survivin has been shown to positively regulate migration in aortic endothelial cells,<sup>26,27</sup> mesenchymal stromal cell,<sup>27</sup> and VSMCs.<sup>28</sup> Notably, one study performed siRNA-mediated knockdown of survivin, which reduced VSMC chemotaxis in a platelet-derived growth factor (PDGF)-driven transwell assay. However, its role in stiffness-mediated VSMC migration remains unknown, so this study aimed to characterize survivin as a potential regulator of this process.

## II. RESULTS

### A. Survivin inhibition reduces both collective and single cell migration on rigid cell culture plates

A previous study found that siRNA-mediated survivin knockdown reduced VSMC chemotaxis in a PDGF-driven transwell assay,<sup>28</sup> suggesting survivin's role in migration, consistent with earlier cancer studies.<sup>29–31</sup> To further test the effects of survivin on both collective and single cell migration of VSMCs, we used sepantronium bromide (YM155) to inhibit survivin, a small molecule survivin inhibitor that has demonstrated selective reduction of survivin expression in various cell types.<sup>32,33</sup> We first confirmed that treating VSMCs with concentrations ranging from 0.1 to 2  $\mu$ M for 24 h effectively reduced survivin levels [Figs. 1(a) and 1(b)], consistent with previous findings.<sup>24,25</sup> We then assessed the impact of survivin inhibition on collective cell migration using a wound-healing assay. VSMCs were cultured to form a monolayer on tissue culture plates, scratched with a micropipette tip, and treated with varying doses of YM155 or DMSO (vehicle control).

Images were taken at 0, 12, and 24 h post-treatment [Fig. 1(c)]. VSMCs treated with DMSO consistently exhibited 60% and 100% wound closure after 12 and 24 h, respectively [Fig. 1(d)]. Meanwhile, cells treated with YM155 showed a dose-dependent decrease in wound closure at both 12 and 24 h compared to DMSO-treated cells. To further assess whether the decrease in cell migration following survivin inhibition is due to reduced proliferation, given our previous findings that survivin inhibition decreases cell proliferation,<sup>24</sup> we treated VSMCs with 10  $\mu$ g/ml Mitomycin C, a proliferation inhibitor,<sup>34–37</sup> and performed a scratch assay. Mitomycin C treatment resulted in approximately a 10% reduction in wound closure; however, this decrease was not statistically significant [Figs. 1(e) and 1(f)], confirming that the wound healing results shown in Fig. 1(c) are primarily not due to changes in proliferation.

Cell–cell contact can influence the speed of cell migration in the wound-healing assay, potentially limiting the information it provides. To investigate the effect of survivin inhibition on individual VSMCs while minimizing cell–cell contact, we conducted a single-cell analysis of VSMC migration. VSMCs were plated on the tissue culture plates at 10%–20% confluency and incubated for 24 h, followed by treatment with DMSO or varying doses of YM155 for 1 h. Time-lapse video microscopy was then performed for 3 h at 3-min intervals, generating a total of 61 images (frames) for each experimental condition. We first confirmed that YM155 treatment in 4 h resulted in reduced survivin protein levels in VSMCs [Figs. 2(a) and 2(b)]. Using Fiji/Image J software, as described previously,<sup>38</sup> we analyzed the images to track nuclear movement frame-by-frame, allowing us to display the cell trajectory and quantify average velocity. Cell trajectory analysis showed that VSMCs treated with YM155 (0.1, 0.5, 1, and 2  $\mu$ M) exhibited significantly decreased average single-cell velocities compared to the control [Figs. 2(c) and 2(d)]. Interestingly, while observing image sequences of individual cells from different experimental groups treated with YM155 or DMSO, we found that survivin-inhibited cells exhibited multiple short protrusions in various directions (loss of directionality), whereas the DMSO-treated control group typically showed a single prolonged protrusion at the leading edge [Fig. 2(e)]. These time-lapse motility observations align with the wound-healing data in Fig. 1 and previous transwell migration data,<sup>28</sup> all indicating that survivin is a key modulator of VSMC migration.

### B. Survivin inhibition reduces stiffness-stimulated cell migration

Substrate stiffness has long been recognized as a critical regulator of cell migration, a process known as durotaxis,<sup>39–48</sup> however, the role of survivin in stiffness-dependent VSMC migration remains unexplored. Here, our results showed that survivin inhibition significantly reduced both collective and single cell migration (Figs. 1 and 2). However, it is important to note that VSMCs were cultured on rigid plastic cell culture dishes, which do not accurately replicate the physiological and pathological stiffness of the *in vivo* environment. To determine whether survivin is required for stiffness-stimulated cell motility, VSMCs were sparsely seeded on fibronectin-coated soft (elastic modulus, 2–8 kPa) and stiff (16–24 kPa) polyacrylamide hydrogels<sup>24,25</sup> for 1 h. The soft hydrogel mimics the physiological stiffness of a healthy mouse femoral artery, while the stiff hydrogel reflects the pathological vessel stiffness seen after vascular injury or

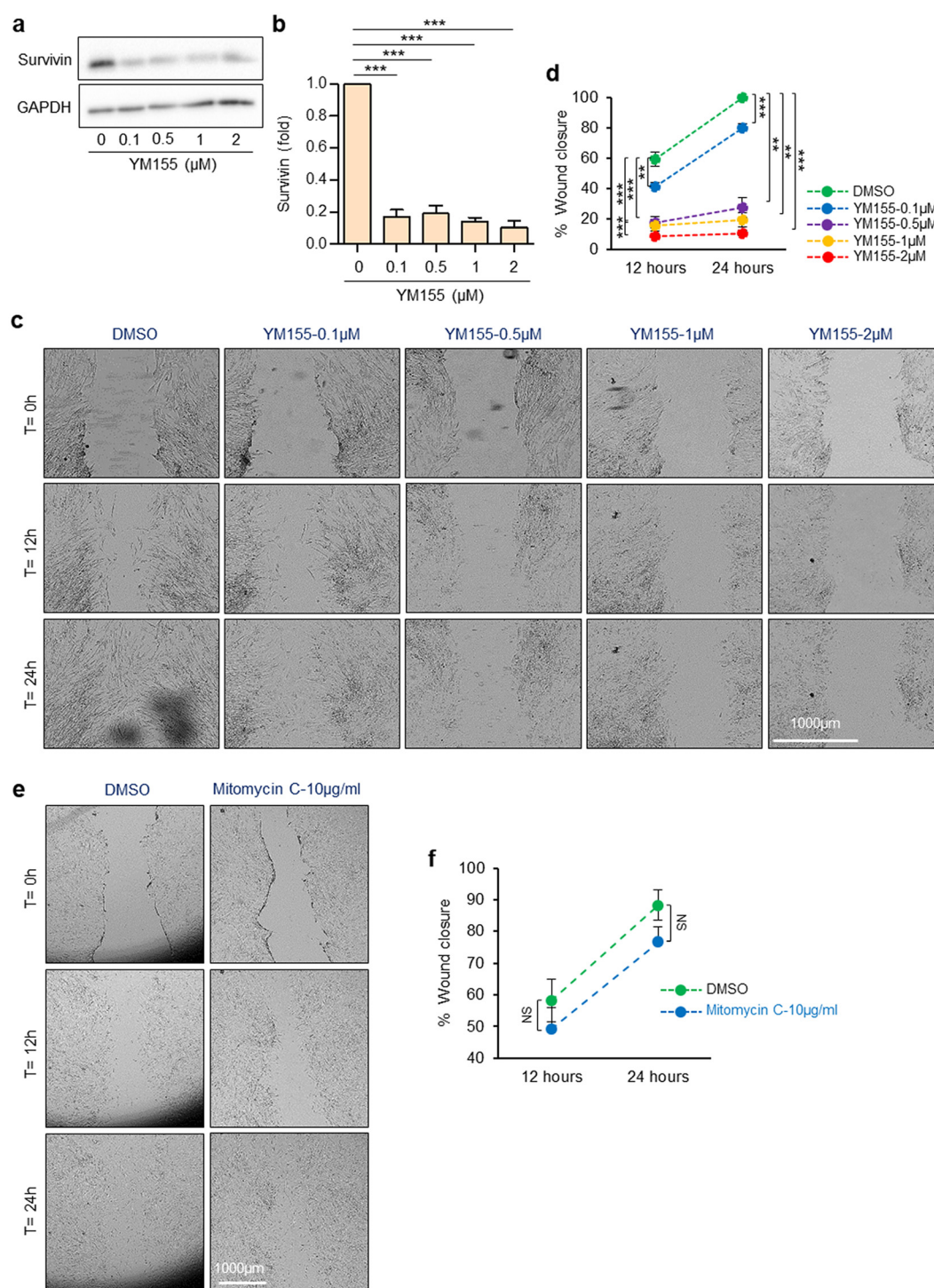


**FIG. 1.** Survivin inhibition reduces collective cell migration. VSMCs plated on cell culture plates were treated with various doses of YM155 (c), 10  $\mu\text{g/ml}$  of Mitomycin C (e), or DMSO (a vehicle control). (a) Total cell lysates were collected for immunoblotting. (b) The graphs show the expression of survivin in VSMCs treated with YM155, normalized to that in VSMCs treated with DMSO.  $n = 5$  independent biological replicates. (c) and (e) A scratch-wound assay was performed, and images were captured at 0, 12, and 24 h post-treatment.  $n = 5$ –12 independent biological replicates (c) and  $n = 5$  independent biological replicates (e). (d) and (f) Wound closure (%) at 12 and 24 h was calculated using the formula:  $[(\text{Initial wound size}) - (\text{wound size at 12 or 24 h})] / (\text{wound size at 12 or 24 h}) \times 100$ .  $^{**}p < 0.01$ ,  $^{***}p < 0.001$ ; ns, not significant.



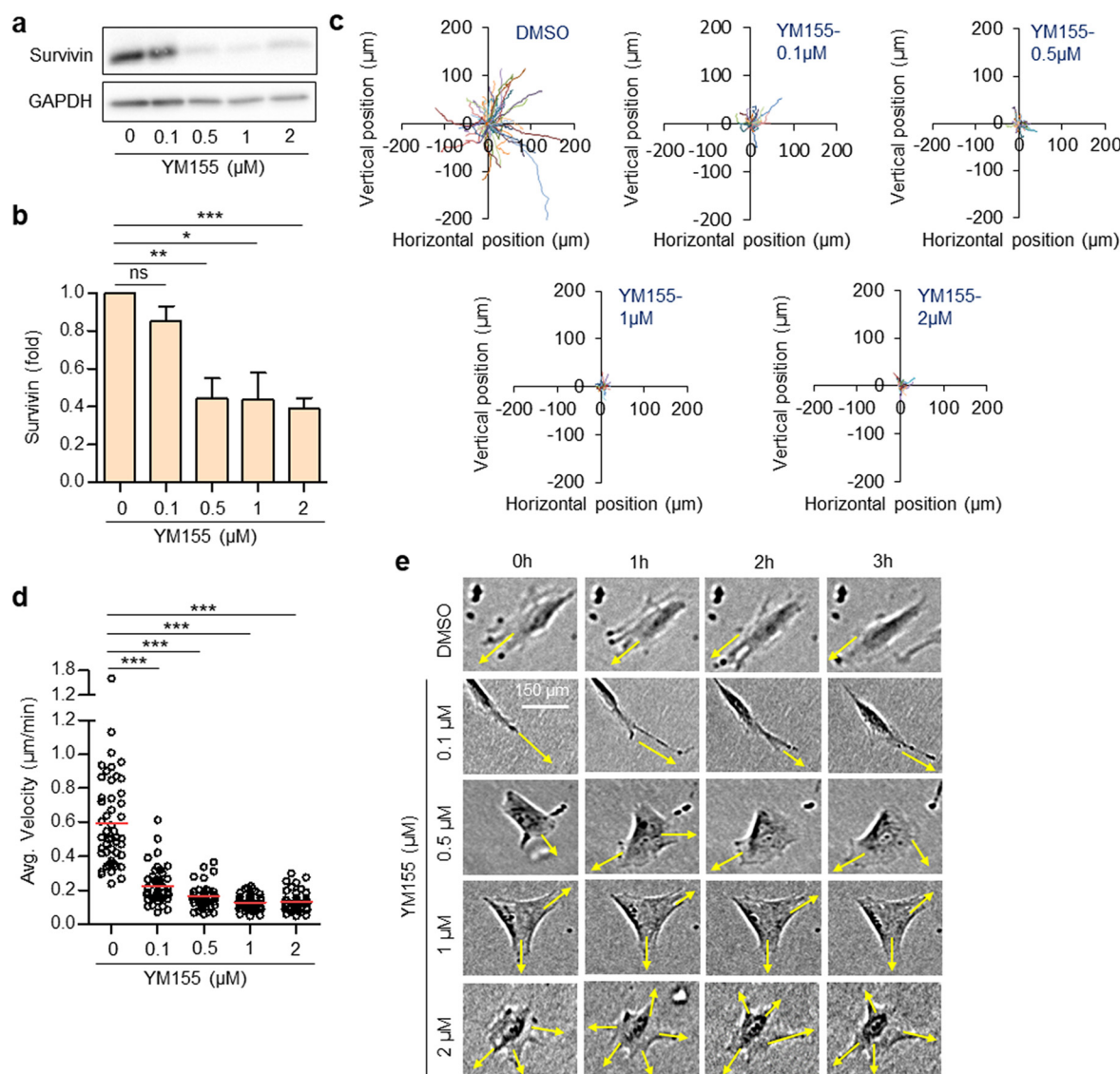


**FIG. 2.** Survivin inhibition decreases single cell migration. (a) VSMCs were sparsely plated on cell culture plates and treated with either YM155 or DMSO for 4 h. Total cell lysates were collected for immunoblotting. (b) The graph shows the expression of survivin in VSMCs treated with varying concentrations of YM155, normalized to that of VSMCs treated with DMSO.  $n = 4$  independent biological replicates. (c)–(e) VSMCs were plated for time-lapse imaging. Manual tracking of these cells was conducted to obtain single-cell trajectories (c) and average cell velocities (d). 49 cells (DMSO), 45 cells (0.1  $\mu\text{M}$  YM155), 42 cells (0.5  $\mu\text{M}$  YM155), 44 cells (1  $\mu\text{M}$  YM155), and 45 cells (2  $\mu\text{M}$  YM155) were analyzed from  $n = 3$  independent biological replicates. (e) Sequences of images from a set of representative time-lapse experiments (arrow-direction of protrusion). \* $p < 0.05$ , \*\* $p < 0.01$ , \*\*\* $p < 0.001$ . ns, not significant.

atherosclerosis.<sup>7,49</sup> Cells were then treated with varying doses of YM155 or DMSO, as described above. After 1 h of treatment, time-lapse video microscopy was performed for 3 h at 3-min intervals, yielding 61 images per condition, which were analyzed using Fiji/Image J software. In addition, cell lysates were collected 4 h after YM155 treatment. We confirmed that survivin expression increases on stiff substrates, as previously shown,<sup>24,25</sup> and that YM155 reduces survivin levels in VSMCs in a dose-dependent manner, attenuating stiffness-mediated survivin expression [Figs. 3(a) and 3(b)]. Single cell trajectory analysis revealed that VSMCs on stiff hydrogels

exhibited significantly greater migration distance [Fig. 3(c)] and speed [Fig. 3(d)], similar to cells on plastic (Fig. 2), compared to those on soft hydrogels. YM155 treatment reduced this increased migration distance and speed to levels similar to those of cells on soft hydrogels. Cells cultured on soft hydrogels displayed a more circular and less spread morphology, as quantified by circularity, and showed fewer protrusions compared to those on stiff hydrogels [Fig. 3(e), supplementary material Fig. 1]. YM155-treated cells on stiff hydrogels displayed moderately more circular morphology and multiple protrusions in varying directions, while DMSO-treated cells

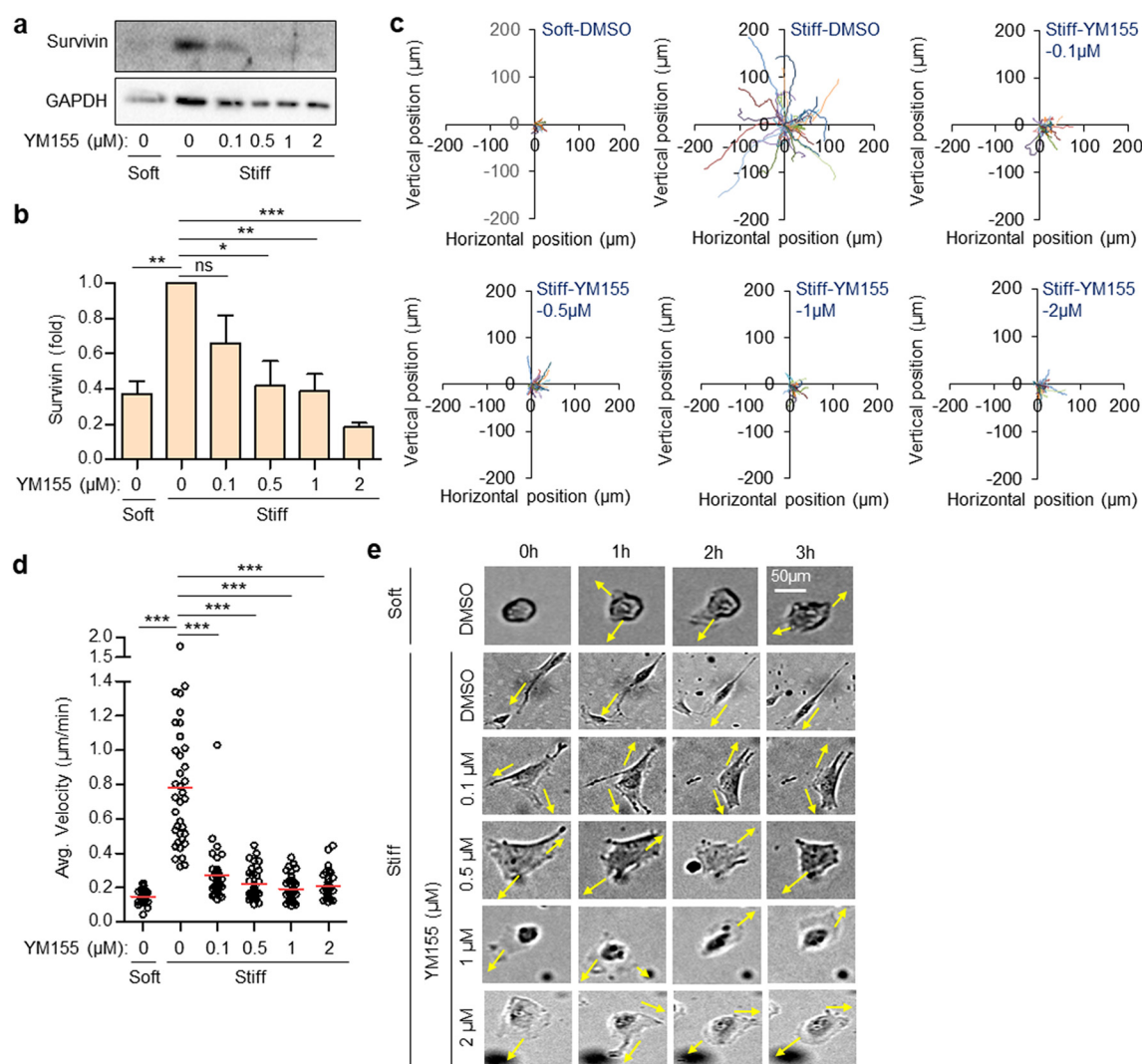


**FIG. 3.** Pharmacological inhibition of survivin reduces stiffness-dependent migration. (a) VSMCs were sparsely seeded on fibronectin-coated soft and stiff hydrogels and treated with YM155 or DMSO for 4 h, followed by collection of total lysates for immunoblotting. (b) The graph shows survivin expression in cells treated with varying concentrations of YM155, normalized to the expression in VSMCs on stiff hydrogels treated with DMSO.  $n = 4$  independent biological replicates. (c)–(e) VSMCs were plated for time-lapse video microscopy, and manual tracking of these cells was conducted to obtain single-cell trajectories (c) and average cell velocities (d). 35 cells (soft-DMSO), 36 cells (stiff-DMSO), 38 cells (stiff-0.1  $\mu\text{M}$  YM155), 39 cells (stiff-0.5  $\mu\text{M}$  YM155), 35 cells (stiff-1  $\mu\text{M}$  YM155), and 35 cells (stiff-2  $\mu\text{M}$  YM155) were analyzed from  $n = 3$  independent biological replicates. (e) Sequences of images from a set of representative time-lapse experiments (arrow-direction of protrusion).  $^*p < 0.05$ ,  $^{**}p < 0.01$ ,  $^{***}p < 0.001$ .

exhibited a single prolonged protrusion at the leading edge [Fig. 3(e), [supplementary material Fig. 1](#)].

To further confirm whether survivin siRNA-mediated knockdown on cell migration yields similar results to those obtained with YM155, we seeded VSMCs transfected with either survivin siRNA or a non-targeting control siRNA on stiff hydrogels. Survivin siRNA reduced survivin expression in VSMCs compared to cells treated with control siRNA [Figs. 4(a) and 4(b)]. Similar to YM155, survivin knockdown significantly reduced stiffness-stimulated cell migration [Figs. 4(c) and 4(d)] and resulted in multiple protrusions [Fig. 4(e)] compared to cells treated with control siRNA. Collectively, these data from YM155 and siRNA

demonstrate that survivin is essential for stiffness-dependent VSMC migration and protrusion.

### C. Survivin inhibition decreases FAK phosphorylation and disrupts actin organization and stress fiber formation

Focal adhesion kinase (FAK) is a key component of the focal adhesion complex, where it regulates adhesion turnover and actin cytoskeletal reorganization, both of which are essential processes for cell motility.<sup>50–52</sup> FAK is activated by phosphorylation at tyrosine 397

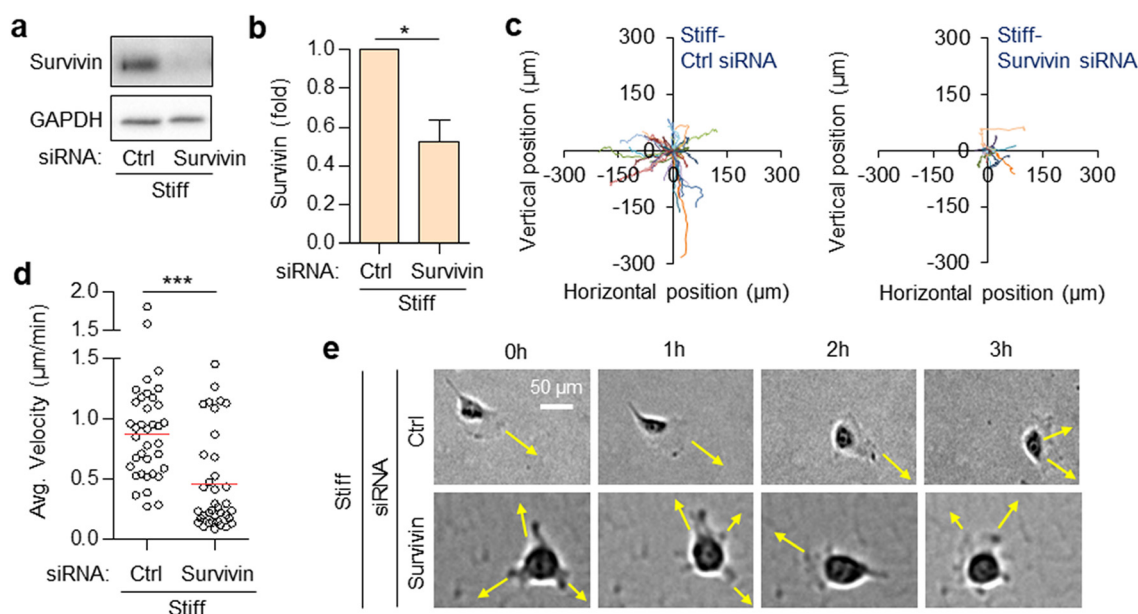


**FIG. 4.** Survivin knockdown decreases stiffness-stimulated cell migration. (a) VSMCs transfected with 200 nM survivin siRNA or non-targeting control siRNA were seeded on fibronectin-coated stiff hydrogels for 4 h. (b) Total cell lysates were analyzed by immunoblotting, and survivin protein levels were normalized to GAPDH.  $n = 3$  independent biological replicates. (c)–(e) VSMCs were plated for time-lapse video microscopy, and manual tracking of these cells was conducted to obtain single-cell trajectories (c) and average cell velocities (d). 37 cells (control siRNA) and 37 cells (survivin siRNA) were analyzed from  $n = 3$  independent biological replicates. (e) Sequences of images from a set of representative time-lapse experiments (arrow-direction of protrusion). \* $p < 0.05$ , \*\*\* $p < 0.001$ .

(FAK<sup>Y397</sup>), which promotes migration<sup>53–55</sup> and this phosphorylation is increased in cells cultured on stiff substrates.<sup>25,56</sup> A previous study showed that recruitment of FAK<sup>Y397</sup> to focal adhesions decreases following survivin inhibition, which partially contributed to reduced cell migration.<sup>57</sup> Inhibition of either FAK phosphorylation<sup>53</sup> or survivin expression<sup>58</sup> also reduces stress fiber formation, a key component of cell migration.<sup>59</sup> To examine whether stiffness and survivin modulate FAK phosphorylation and the actin cytoskeleton, we seeded VSMCs treated with YM155 on soft or stiff hydrogels for <24 h prior to immunostaining for FAK<sup>Y397</sup> and actin (Fig. 5). The number of FAK<sup>Y397</sup> clusters was counted as previously described.<sup>57,60</sup> Our data showed that significantly more FAK<sup>Y397</sup> clusters were present on stiff hydrogels compared to soft ones [Fig. 5(b)]. Moreover, survivin inhibition led to a dose-dependent reduction in FAK<sup>Y397</sup> clusters at focal adhesions [Figs. 5(a) and 5(b)]. We also found that cells on stiff hydrogels exhibited a more organized actin network and increased stress fiber formation relative to those on soft hydrogels, consistent with previous findings<sup>25,61</sup> [Fig. 5(a)]. Survivin inhibition disrupted actin organization and stress fiber formation in a dose-dependent manner [Fig. 5(a)]. These findings suggest that survivin regulates stiffness-dependent cell migration by regulating FAK phosphorylation and actin cytoskeletal dynamics.

#### D. Survivin overexpression increases cell migration on soft hydrogels

Survivin protein levels are higher on stiff hydrogels, and cells exhibit greater migratory behavior compared to those on soft hydrogels. To determine whether survivin overexpression alone is sufficient

to induce cell migration on soft hydrogels, we infected VSMCs with adenoviruses encoding wild-type survivin or green fluorescent protein (GFP) control [Figs. 6(a) and 6(b)] and then plated them on soft hydrogels for time-lapse video microscopy. VSMCs infected with adenoviral GFP exhibited a migration rate of 0.169  $\mu\text{m}/\text{min}$ . VSMCs treated with adenoviral survivin at 25 and 50 MOI displayed migration rates of 0.249 and 0.337  $\mu\text{m}/\text{min}$ , respectively [Figs. 6(c) and 6(d)]. Survivin overexpression increased directional persistence with a prolonged protrusion at the leading edge [Fig. 6(e)]. Collectively, these findings suggest that while survivin partially rescues cell motility and protrusion behaviors under soft conditions, substrate stiffness is still required to fully restore the cell migration observed on stiff conditions.

#### III. DISCUSSION

Survivin has been associated with the progression of neointimal hyperplasia,<sup>17,19</sup> hypertension,<sup>22</sup> and atherosclerosis,<sup>18</sup> conditions characterized by increased arterial stiffness. Notably, survivin inhibition reduced neointimal hyperplasia in vascular injury models of both mice and rabbits by regulating VSMC migration and proliferation.<sup>17,19</sup> More recently, we showed that survivin is highly expressed under stiff conditions, where it promotes VSMC proliferation, intracellular stiffness, and ECM synthesis.<sup>24,25</sup> However, its role in stiffness-stimulated VSMC motility remains uncharacterized, and this study is the first to characterize survivin as a key mechano-sensitive regulator. Our data demonstrate that stiffness and survivin cooperatively increase cell migration, likely through increased cell spreading and protrusion—processes essential for extending the leading edge, forming new focal adhesions to ECM, and facilitating cell motility.<sup>62,63</sup> VSMC on stiff hydrogels showed increased spreading and directional migration



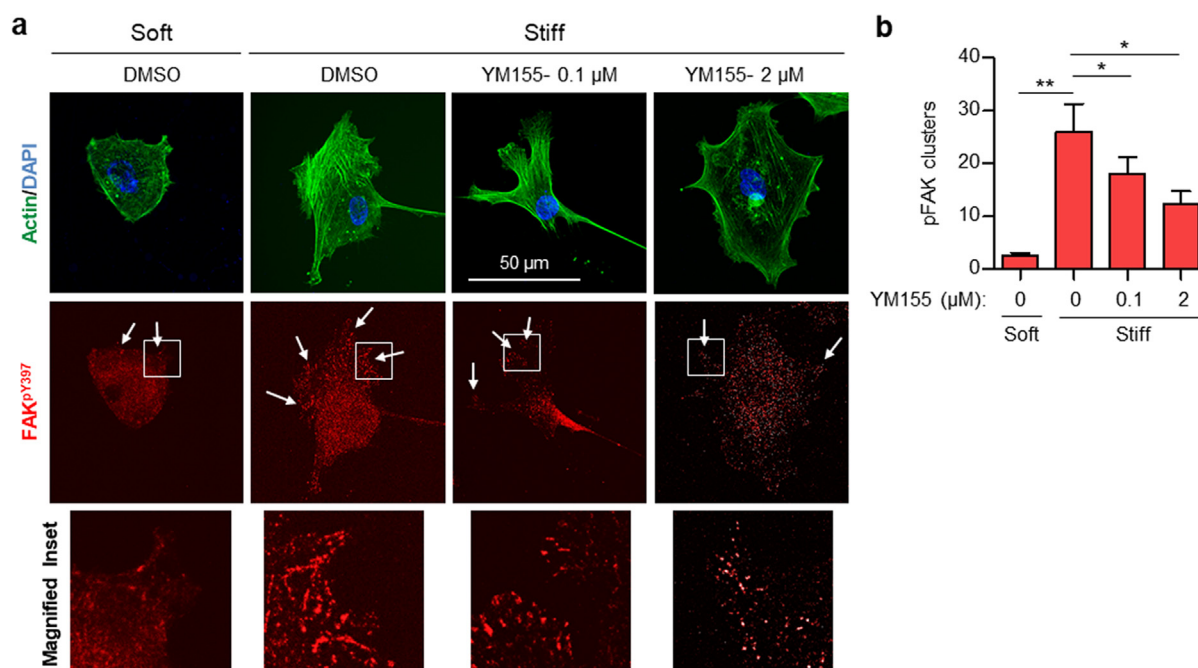


**FIG. 5.** Survivin regulates FAK phosphorylation, actin organization, and stress fiber formation. (a) VSMCs were sparsely seeded on fibronectin-coated soft and stiff hydrogels and treated with either YM155 or DMSO. Cells were stained with DAPI, phospho-FAK (Tyr397) antibody and Alexa Fluor 647-phalloidin. Fluorescence images were acquired using a spinning disk confocal microscope with a 63 $\times$  oil-immersion objective. The outlined boxes indicate the regions shown in the magnified insets. (b) A sum of slices projection of each cell was generated using Fiji/ImageJ, and FAK<sup>pY397</sup> clusters were manually counted. 37 cells (soft-DMSO), 44 cells (stiff-DMSO), 33 cells (stiff-0.1  $\mu$ M YM155), and 37 cells (stiff-2  $\mu$ M YM155) were analyzed from  $n = 3$  independent biological replicates. \* $p < 0.05$ , \*\* $p < 0.01$ .

compared to those on soft hydrogels, aligning with observations from Rickel *et al.*<sup>64</sup> and our current (Fig. 3, supplementary material Fig. 1) and prior studies.<sup>24</sup> On soft hydrogels, VSMCs exhibited more circular morphology and formed multiple short protrusions without a defined leading edge, reducing directional migration, whereas cells on stiff hydrogels typically displayed more elongated morphology and formed a single prolonged protrusion at the leading edge, increasing directional migration. These stiffness-induced increases in cell motility and spreading were significantly attenuated by survivin inhibition, resulting in a protrusion phenotype resembling that observed on soft hydrogels. Our findings align with earlier work by Nabzdyk *et al.* which linked survivin to VSMC motility using a transwell assay, although their study did not account for physiological stiffness conditions.<sup>28</sup> Furthermore, survivin overexpression on soft hydrogels partially rescued migration, with fewer protrusions and increased spreading.<sup>24</sup> These results suggest that both ECM stiffness and survivin expression are required to recapitulate the migratory phenotype observed under stiff conditions. Importantly, the observed effect was not a consequence of reduced cell proliferation [Fig. 1(e)].

Given that both collective and single-cell migration contribute to neointimal hyperplasia and formation,<sup>65,66</sup> we examined both modes of migration in our study. Previous studies have shown that cell-cell interactions by mediated by junctional proteins, such as n-cadherin facilitate collective cell migration.<sup>67,68</sup> However, in response to vascular injury, the phenotypic switch of VSMCs from a contractile to a synthetic state at the injured regions often leads to the disruption or loss of adherent junctions,<sup>69</sup> weakening cell-cell adhesion and enabling

individual cell migration, as observed in our findings [see wound healing image of DMSO-treated cells at the 12- and 24-h time points in Figs. 1(c) and 1(e)] and supported by a previous study.<sup>66</sup> While collective cell migration is regarded as the key driver for vascular remodeling, a process central to neointima formation, the presence or absence of stable cell-cell junctions may determine whether cells migrate collectively or individually.<sup>70</sup> Taken together, our data and previous findings suggest that the both collective and single-cell migration contribute to the progression and development of neointima.

The mechanism by which survivin regulates stiffness-dependent VSMC migration remains underexplored. One potential pathway involves FAK, which plays a critical role in focal adhesion dynamics and actin cytoskeleton organization, both essential for cell motility.<sup>51,52</sup> Previous studies have shown that phosphorylation of FAK at Tyr 397 (FAK<sup>pY397</sup>) is essential for cell protrusion and migration<sup>53–55</sup> and is increased under stiff conditions.<sup>25,56</sup> In prostate cancer cells, survivin inhibition was reported to reduce migration, partly due to decreased FAK<sup>pY397</sup> levels at focal adhesions.<sup>57</sup> This effect was likely driven by reduced recruitment of FAK<sup>pY397</sup> to focal adhesions complexes, leading to diminished cell protrusion. Indeed, survivin inhibition in VSMCs decreased FAK<sup>pY397</sup> recruitment to focal adhesions under stiff conditions [Fig. 5(b)], in line with our immunoblotting data showing reduced FAK<sup>pY397</sup> levels following YM155 treatment.<sup>25</sup> Inhibition of FAK<sup>pY397</sup> was shown to reduce actin stress fiber formation.<sup>53</sup> Stress fibers interact with focal adhesions,<sup>71</sup> establish cell polarity,<sup>72</sup> and play a crucial role in mechanotransduction<sup>73</sup> by enabling cells to sense substrate stiffness and regulate cell migration.<sup>59</sup> Several studies

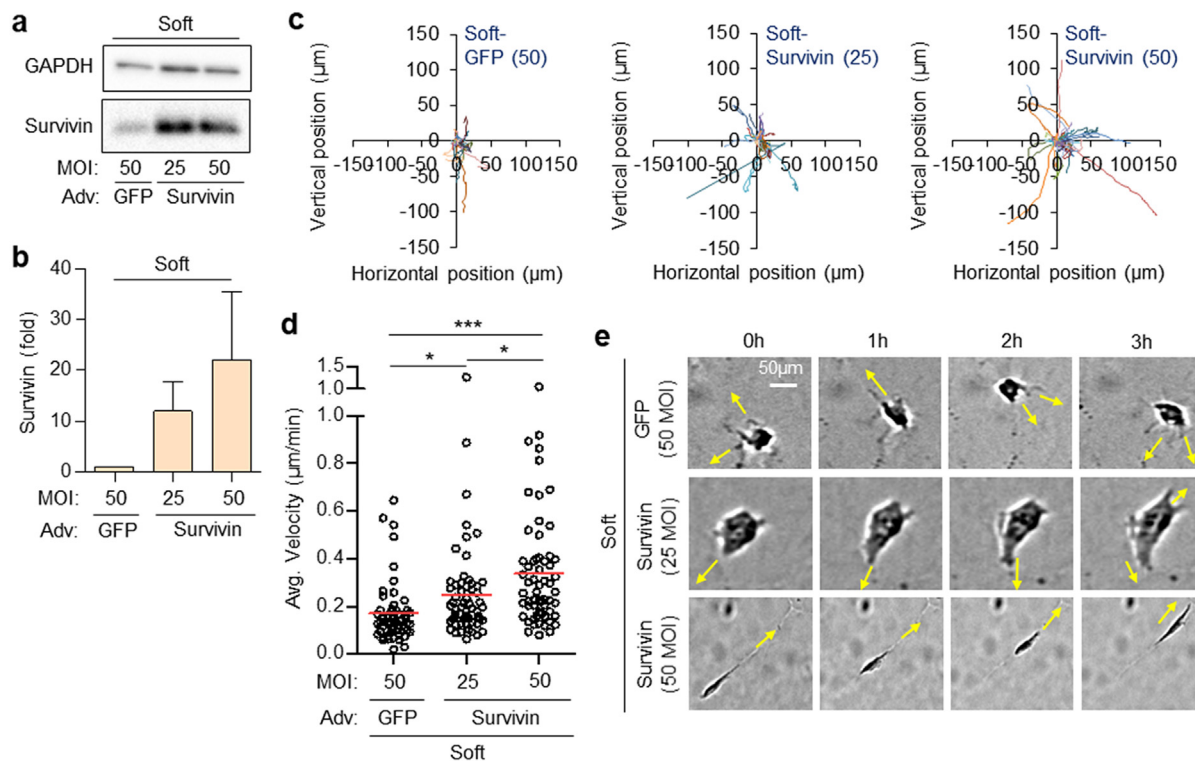


**FIG. 6.** Survivin overexpression partially rescues cell migration on soft hydrogels. (a) VSMCs were infected with either adenoviral GFP (50 MOI) or survivin (25 and 50 MOI). (b) Total cell lysates were analyzed by immunoblotting, and survivin protein levels were normalized to GAPDH.  $n = 3$  independent biological replicates. (c)–(e) VSMCs were plated for time-lapse video microscopy, and manual tracking of these cells was conducted to obtain single-cell trajectories (c) and average cell velocities (d). 59 cells (GFP 50 MOI), 60 cells (survivin 25 MOI), and 60 cells (survivin 50 MOI) were analyzed from  $n = 5$  independent biological replicates. (e) Sequences of images from a set of representative time-lapse experiments (arrow-direction of protrusion). \* $p < 0.05$ , \*\*\* $p < 0.001$ . ns, not significant.

demonstrated that survivin inhibition significantly disrupted actin cytoskeleton and stress fiber formation,<sup>58,74</sup> which is consistent with our findings in VSMCs under stiff conditions. Taken together, our results and previous findings suggest that survivin regulates stiffness-dependent migration by modulating FAK phosphorylation, which, in turn, influences focal adhesion dynamics and actin cytoskeleton organization.

ECM proteins, including collagen-1, lysyl oxidase (Lox), and fibronectin, are also key regulators of cell migration and major contributors to the progression of various CVDs and related pathologies.<sup>25,75</sup> Differentiated VSMCs synthesize and deposit these ECM proteins, which contribute to arterial stiffening. Our recent study demonstrated a stiffness-dependent increase in collagen-1, fibronectin, and Lox expression and deposition by VSMCs, which was attenuated by survivin inhibition.<sup>25</sup> Other studies have shown that inhibiting newly synthesized collagen in porcine arterial SMCs reduces migration,<sup>76</sup> while fibronectin induces a phenotypic switch that promotes migration.<sup>77,78</sup> Additionally, Lox inhibition has been shown to reduce atherosclerotic formation and the restenotic process, potentially by decreasing VSMC migration and proliferation.<sup>77,79</sup> Therefore, another potential mechanism by which survivin may modulate stiffness-dependent VSMC migration is by regulating the expression of ECM proteins.

Our previous study identified survivin as a key mediator of stiffness-dependent VSMC proliferation by regulating the expression of

cyclin D1, a major driver of cell cycle progression.<sup>24</sup> Interestingly, a previous study showed that cyclin D1 promotes migration of mouse embryonic fibroblasts by inhibiting Rho-activated kinase signaling.<sup>80–82</sup> Additionally, cyclin D1 interacts with and positively regulates filamin A, a cytoskeleton protein involved in cell migration.<sup>82</sup> In pulmonary arterial SMCs, inhibition of filamin A reduces cell motility.<sup>83</sup> Thus, survivin-induced cyclin D1 expression may influence filamin A function, thereby facilitating cell migration.

#### IV. CONCLUSION

Understanding the molecular mechanisms driving aberrant cellular behaviors is critical for developing therapeutic strategies for stiffness-associated cardiovascular diseases. Our findings highlight the role of survivin in migration under pathological stiffness conditions, offering insight into the molecular pathways linking ECM stiffness to cardiovascular pathology.

#### V. METHODS

##### A. Cell culture

Human vascular smooth muscle cells (VSMCs; catalog number [Cat. No.] 354-05a, Cell Applications, Inc.) were cultured in Dulbecco's modified Eagle's medium (DMEM; Cat. No. 10-014-CV, Corning) supplemented with 10% fetal bovine serum (FBS; Cat. No. 2510268RP, GIBCO), 1 mM sodium pyruvate (Cat. No. S8636, Sigma-



Aldrich), 1% penicillin–streptomycin (Cat. No. 30-002-CI, Corning), 50 µg/ml gentamicin (Cat. No. 30-005-CR, Corning), and 2% minimum essential media (MEM) amino acids (Cat. No. M5550, Sigma-Aldrich). The cells were maintained at 37 °C and 10% CO<sub>2</sub> and used up to passage 5. To ensure optimal cell growth, the culture medium was replaced every 2–3 days, and the cells were passaged at 80%–90% confluency.

## B. Drug treatment

VSMCs were plated on plastic cell culture plates, glass coverslips, or soft and stiff hydrogels in media containing 10% serum with varying doses (0.1, 0.5, 1, or 2 µM) of YM155 (survivin inhibitor; Cat. No. 11490, Cayman Chemical), 10 µg/ml Mitomycin C (proliferation inhibitor; Cat. No. BML-GR311-0002, Enzo Life Sciences), or dimethyl sulfoxide (DMSO; Cat. No. D8418, Sigma-Aldrich) as a vehicle control. VSMCs were incubated with the drug for a predetermined period before being used in assays to assess the impact of YM155 on the cells.

## C. Preparation of polyacrylamide hydrogels

Soft (2–8 kPa) and stiff (18–24 kPa) fibronectin-coated polyacrylamide hydrogels, designed to mimic the physiological stiffness of normal (soft) and diseased/injured arteries (stiff), were used, with their stiffness previously measured using atomic force microscopy.<sup>24,25,49,56,84</sup> Briefly, autoclaved glass coverslips were etched with 1.0 M sodium hydroxide for 3 min, then treated with 3-(trimethoxysilyl)propyl methacrylate (Cat. No. 440159, Sigma-Aldrich) to introduce amine groups for cross-linking with hydrogel. Hydrogel solution was prepared by mixing a solution of a pre-determined ratio<sup>85</sup> of 40% acrylamide (Cat. No. 1610148, Bio-Rad) and 1% bis-acrylamide (Cat. No. 1610142, Bio-Rad) with sterile water, 10% ammonium persulfate (Cat. No. A3678, Sigma-Aldrich), Tetramethylethylenediamine (TEMED; Cat. No. J63734, AC, Thermo Fisher Scientific), and a solution of N-hydroxysuccinimide (NHS; Cat. No. A8060, Sigma-Aldrich)-fibronectin (Cat. No. 341631, Calbiochem). The NHS–fibronectin solution was prepared by combining fibronectin (100 µl at 1 mg/ml dissolved in 1.9 ml Tris base solution at pH 8.4) with 222 µl of 1 mg/ml NHS (dissolved in 1 ml of DMSO) and incubated at 37 °C for 1 h. The solution was then dispensed on the etched/methacrylate-treated glass coverslip, and a siliconized glass coverslip [prepared using 20% Surfasil (Cat. No. TS42801, Thermo Fisher Scientific) in 80% chloroform (Cat. No. J67241.AP, Thermo Fisher Scientific)] was placed on top of the dispensed solution. The polymerized hydrogels were extensively washed with Dulbecco's phosphate-buffered saline (DPBS) to remove unpolymerized polyacrylamide and were blocked with 1 mg/ml heat-inactivated, fatty-acid-free bovine serum albumin (BSA) for 1 h.

## D. Wound-healing assay

VSMCs were seeded on a cell culture plate, and once the cells reached confluence, a scratch was made down the middle of the monolayer using a p200 micropipette tip. The cells were rinsed once with warm DPBS and incubated in DMEM containing YM155 or DMSO. Additionally, in a separate experiment, VSMCs were pretreated with 10 µg/ml Mitomycin C or DMSO for 2 h before scratch wounding, as described previously.<sup>34–37</sup> Images were obtained with Cytation 1 or Cytation 5 Imaging Multimode Readers (Agilent Technologies, Inc.).

To analyze the results of these assays, images at  $t=0$ ,  $t=12$ , and  $t=24$  h were used. The visible wound in the cell monolayer was manually annotated, and the wound area in each image was measured. The percent of wound closure after 24 h was subsequently calculated.

## E. Time-lapse single-cell motility assay and image analysis

VSMCs were seeded at 20%–30% confluency on cell culture plates or polyacrylamide hydrogels to minimize cell–cell contact and incubated overnight. Following incubation, cells were treated with YM155 or DMSO and immediately placed in a Cytation 1 Imaging Multimode Reader for time-lapse imaging at 37 °C and 10% CO<sub>2</sub>. Images were captured every 3 min for 3 h to track cell migration. The time-lapse images were analyzed using Fiji/ImageJ to determine cell migration distance and speed, as previously described.<sup>38</sup> Cell trajectory was constructed by manually marking frame-by-frame the centroid positions (x, y) of cell nuclei. Note that dividing or touching cells were excluded from the analysis.

## F. siRNA transfection and adenovirus infection

VSMCs were transfected with 100 nM survivin (Cat. No. AM16704, Ambion) or control siRNA (ID No. 121294, Ambion) using Lipofectamine 3000 reagent (Cat. No. L3000-015, Invitrogen) in Opti-MEM reduced serum media (Cat. No. 31985-070, Gibco) as previously described.<sup>86</sup> Five hours after siRNA transfection, cells were serum starved in DMEM containing 1 mg/ml BSA for 48 h, then plated on soft and stiff hydrogels, with experiments performed within 24 h. Survivin siRNA sequence is 5'-CCACUCCAGGGUUAUUCtt-3'. For adenovirus infection, VSMCs were infected for 24 h with adenoviruses encoding wild-type survivin [multiplicity of infection (MOI), 25 and 50; Cat. No. 1611, Vector Biolabs] or GFP (MOI 50; Cat. No. 1060, Vector Biolabs), with GFP serving as the experimental control. Following incubation, cells were plated on soft and stiff hydrogels for experiments.

## G. Protein extraction and immunoblotting

Total cell lysates were collected from VSMCs cultured on soft and stiff hydrogels as described previously.<sup>56</sup> Cells were first lysed by placing hydrogels face-down on warm 5× sample buffer (250 mM Tris [pH 6.8], 10% SDS, 50% glycerol, 0.2% bromophenol blue, and 10 mM 2-mercaptoethanol) for 2 min at room temperature. For immunoblotting, equal amounts of extracted protein were fractionated on 12% SDS-polyacrylamide gels, and the fractionated proteins were transferred electrophoretically to a polyvinylidene fluoride (PVDF; Cat. No. 10026933, Bio-Rad) membrane using the Trans-Blot Turbo Transfer System (Bio-Rad). The PVDF membrane was blocked in 5% milk in TBST (Tris-buffered saline with 0.1% Tween 20 detergent) for 1 h at room temperature, then incubated with primary antibodies against survivin (1:250; Cat. No. 71G4B7, Cell Signaling Technology) and GAPDH (1:10 000; Cat. No. 60004-1-Ig, Proteintech) diluted in 5% milk in TBST for 2 h at room temperature, overnight at 4 °C, and an additional 2 h at room temperature followed by a 30-min wash with TBST. The membranes were then probed with the secondary antibody, horseradish peroxidase (HRP)-conjugated Goat Anti-Rabbit IgG (H + L) (1:1000; Cat. No. SA00001-2, Proteintech), diluted in 5% milk in TBST for 1 h at room temperature, then washed three times with

TBST. Antibody signals were detected using Clarity (Cat. No. 170561, Bio-Rad) or Clarity Max (Cat. No. 1705062, Bio-Rad) Western ECL substrates on ChemiDoc XRS+ imaging system and band intensity was analyzed using ImageJ.

## H. Immunostaining and image analysis

For cell morphology analysis, VSMCs seeded on soft or stiff hydrogels were treated with 0.1 or 2  $\mu$ M YM155 or DMSO, for <24 h. Cells were fixed with 3.7% formaldehyde for 1 h, permeabilized with 0.4% Triton X-100 for 40 min, blocked with 5% BSA for 1 h, and incubated with Alexa Fluor 647-phalloidin (1:200; Cat. No. A22287, Thermo Fisher Scientific) and DAPI (Cat. No. D1306, Thermo Fisher Scientific). Fluorescence images were acquired using a Leica DMi8 inverted or DM6B upright microscope with a 10 $\times$  objective and analyzed using Fiji/ImageJ to measure circularity. Dividing or touching cells were excluded from the analysis.

For phospho-FAK clustering assay, the same experimental procedures and conditions were used as described above, except cells were stained with phospho-FAK (Tyr397) antibody (1:25; Cat. No. 3283, Cell Signaling Technology) and Alexa Fluor 647-phalloidin (1:200; Cat. No. A22287, Thermo Fisher Scientific). Fluorescence images were acquired using an Okolab 3i spinning disk confocal microscope with a 63 $\times$  oil-immersion objective. A sum of slices projection of each cell was generated using Fiji/ImageJ, and FAK<sup>pY397</sup> clusters were manually counted.

## I. Statistical analysis

Data are presented as the mean  $\pm$  standard error of the mean (SEM). As appropriate, the statistical analysis was performed using a Student's t-test or a one-way ANOVA. Results with P-values less than 0.05 (\*), 0.01 (\*\*), or 0.001 (\*\*\*) were considered to be statistically significant.

## SUPPLEMENTARY MATERIAL

See the [supplementary material](#) (supplementary Fig. 1) for additional information.

## ACKNOWLEDGMENTS

This work was supported by an NIH/NHLBI Grant No. R01HL163168 to Y.B. and an NIGMS Grant No. R35GM156870 to A.T.L.

## AUTHOR DECLARATIONS

### Conflict of Interest

The authors have no conflicts to disclose.

### Ethics Approval

Ethics approval is not required.

### Author Contributions

Thomas Mousso and Kalina Rice contributed equally to this work.

**Thomas Mousso:** Conceptualization (lead); Data curation (supporting); Formal analysis (supporting); Investigation (lead); Methodology

(equal); Writing – original draft (equal); Writing – review & editing (equal). **Kalina Rice:** Conceptualization (lead); Data curation (lead); Formal analysis (lead); Investigation (lead); Methodology (lead); Writing – original draft (equal); Writing – review & editing (equal). **Bat-Ider Tumenbayar:** Formal analysis (supporting); Investigation (supporting); Methodology (supporting); Visualization (supporting); Writing – review & editing (supporting). **Khanh Pham:** Investigation (supporting); Writing – original draft (supporting); Writing – review & editing (supporting). **Yuna Heo:** Formal analysis (supporting); Methodology (supporting); Writing – review & editing (supporting). **Su Chin Heo:** Conceptualization (supporting); Writing – review & editing (supporting). **Kwonmoo Lee:** Conceptualization (supporting); Methodology (supporting); Writing – review & editing (supporting). **Andrew T. Lombardo:** Conceptualization (supporting); Writing – review & editing (supporting). **Yongho Bae:** Conceptualization (lead); Investigation (supporting); Methodology (supporting); Project administration (lead); Resources (lead); Supervision (lead); Validation (supporting); Writing – original draft (lead); Writing – review & editing (lead).

## DATA AVAILABILITY

The data that support the findings of this study are available from the corresponding author upon reasonable request.

## REFERENCES

- <sup>1</sup>H. L. Kim, “Arterial stiffness and hypertension,” *Clin. Hypertens.* **29**, 31 (2023).
- <sup>2</sup>K. Pakk *et al.*, “A novel CD147 inhibitor, SP-8356, reduces neointimal hyperplasia and arterial stiffness in a rat model of partial carotid artery ligation,” *J. Transl. Med.* **17**, 274 (2019).
- <sup>3</sup>Y. Chen, F. Shen, J. Liu, and G. Y. Yang, “Arterial stiffness and stroke: Destiffening strategy, a therapeutic target for stroke,” *Stroke Vasc. Neurol.* **2**, 65–72 (2017).
- <sup>4</sup>C. Palombo and M. Kozakova, “Arterial stiffness, atherosclerosis and cardiovascular risk: Pathophysiologic mechanisms and emerging clinical indications,” *Vasc. Pharmacol.* **77**, 1–7 (2016).
- <sup>5</sup>M. O. J. Grootaert and M. R. Bennett, “Vascular smooth muscle cells in atherosclerosis: Time for a re-assessment,” *Cardiovasc. Res.* **117**, 2326–2339 (2021).
- <sup>6</sup>S. O. Marx, H. Totary-Jain, and A. R. Marks, “Vascular smooth muscle cell proliferation in restenosis,” *Circulation* **4**, 104–111 (2011).
- <sup>7</sup>D. Kothapalli *et al.*, “Cardiovascular protection by ApoE and ApoE-HDL linked to suppression of ECM gene expression and arterial stiffening,” *Cell Rep.* **2**, 1259–1271 (2012).
- <sup>8</sup>A. C. Aprotosoaie, A. D. Costache, and I. I. Costache, “Therapeutic strategies and chemoprevention of atherosclerosis: What do we know and where do we go?,” *Pharmaceutics* **14**, 722 (2022).
- <sup>9</sup>E. Shlofmitz, M. Iantorno, and R. Waksman, “Restenosis of drug-eluting stents: A new classification system based on disease mechanism to guide treatment and state-of-the-art review,” *Circulation* **12**, e007023 (2019).
- <sup>10</sup>J. D. Abbott, “Revealing the silver and red lining in drug-eluting stents with angiography,” *Circulation* **1**, 7–9 (2008).
- <sup>11</sup>A. V. Finn *et al.*, “Vascular responses to drug eluting stents: Importance of delayed healing,” *Arterioscler. Thromb. Vasc. Biol.* **27**, 1500–1510 (2007).
- <sup>12</sup>I. Iakovou *et al.*, “Incidence, predictors, and outcome of thrombosis after successful implantation of drug-eluting stents,” *JAMA* **293**, 2126–2130 (2005).
- <sup>13</sup>H. Garg, P. Suri, J. C. Gupta, G. P. Talwar, and S. Dubey, “Survivin: A unique target for tumor therapy,” *Cancer Cell Int.* **16**, 49 (2016).
- <sup>14</sup>Y. Cao *et al.*, “Targeting survivin with Tanshinone IIA inhibits tumor growth and overcomes chemoresistance in colorectal cancer,” *Cell Death Discovery* **9**, 351 (2023).
- <sup>15</sup>J. A. McKenzie and D. Grossman, “Role of the apoptotic and mitotic regulator survivin in melanoma,” *Anticancer Res.* **32**, 397–404 (2012).

- <sup>16</sup>G. Ambrosini, C. Adida, and D. C. Altieri, "A novel anti-apoptosis gene, survivin, expressed in cancer and lymphoma," *Nat. Med.* **3**, 917–921 (1997).
- <sup>17</sup>H. F. Simosa *et al.*, "Survivin expression is up-regulated in vascular injury and identifies a distinct cellular phenotype," *J. Vasc. Surg.* **41**, 682–690 (2005).
- <sup>18</sup>O. P. Blanc-Brude *et al.*, "IAP survivin regulates atherosclerotic macrophage survival," *Arterioscler. Thromb. Vasc. Biol.* **27**, 901–907 (2007).
- <sup>19</sup>Y. Xu *et al.*, "Inhibition of neointimal hyperplasia in rats treated with atorvastatin after carotid artery injury may be mainly associated with down-regulation of survivin and Fas expression," *Pharm. Biol.* **52**, 1196–1203 (2014).
- <sup>20</sup>P. J. Lee *et al.*, "Survivin gene therapy attenuates left ventricular systolic dysfunction in doxorubicin cardiomyopathy by reducing apoptosis and fibrosis," *Cardiovasc. Res.* **101**, 423–433 (2014).
- <sup>21</sup>G. J. Wang *et al.*, "Regulation of vein graft hyperplasia by survivin, an inhibitor of apoptosis protein," *Arterioscler. Thromb. Vasc. Biol.* **25**, 2081–2087 (2005).
- <sup>22</sup>M. S. McMurtry *et al.*, "Gene therapy targeting survivin selectively induces pulmonary vascular apoptosis and reverses pulmonary arterial hypertension," *J. Clin. Invest.* **115**, 1479–1491 (2005).
- <sup>23</sup>O. P. Blanc-Brude *et al.*, "Inhibitor of apoptosis protein survivin regulates vascular injury," *Nat. Med.* **8**, 987–994 (2002).
- <sup>24</sup>J. C. Biber *et al.*, "Survivin as a mediator of stiffness-induced cell cycle progression and proliferation of vascular smooth muscle cells," *APL Bioeng.* **7**, 046108 (2023).
- <sup>25</sup>A. Krajcnik *et al.*, "Survivin regulates intracellular stiffness and extracellular matrix production in vascular smooth muscle cells," *APL Bioeng.* **7**, 046104 (2023).
- <sup>26</sup>H. Zhang *et al.*, "Pleiotropic effects of survivin in vascular endothelial cells," *Microvasc. Res.* **108**, 10–16 (2016).
- <sup>27</sup>Z. Li *et al.*, "Effects of survivin on angiogenesis in vivo and in vitro," *Am. J. Transl. Res.* **8**, 270–283 (2016).
- <sup>28</sup>C. S. Nabzdyk, H. Lancero, K. P. Nguyen, S. Salek, and M. S. Conte, "RNA interference-mediated survivin gene knockdown induces growth arrest and reduced migration of vascular smooth muscle cells," *Am. J. Physiol. Heart Circ. Physiol.* **301**, H1841–H1849 (2011).
- <sup>29</sup>J. A. McKenzie, T. Liu, A. G. Goodson, and D. Grossman, "Survivin enhances motility of melanoma cells by supporting Akt activation and  $\alpha 5$  integrin upregulation," *Cancer Res.* **70**, 7927–7937 (2010).
- <sup>30</sup>C. J. Tai *et al.*, "Survivin-mediated cancer cell migration through GRP78 and epithelial-mesenchymal transition (EMT) marker expression in Mchavlu cells," *Ann. Surg. Oncol.* **19**, 336–343 (2012).
- <sup>31</sup>X. Chen, N. Duan, C. Zhang, and W. Zhang, "Survivin and tumorigenesis: Molecular mechanisms and therapeutic strategies," *J. Cancer* **7**, 314–323 (2016).
- <sup>32</sup>Y. Voges *et al.*, "Effects of YM155 on survivin levels and viability in neuroblastoma cells with acquired drug resistance," *Cell Death Dis.* **7**, e2410 (2016).
- <sup>33</sup>X. J. Cheng *et al.*, "Survivin inhibitor YM155 suppresses gastric cancer xenograft growth in mice without affecting normal tissues," *Oncotarget* **7**, 7096–7109 (2016).
- <sup>34</sup>L. Chen, S. Guo, M. J. Ranzer, and L. A. DiPietro, "Toll-like receptor 4 has an essential role in early skin wound healing," *J. Invest. Dermatol.* **133**, 258–267 (2013).
- <sup>35</sup>M. J. Simpson *et al.*, "Quantifying the roles of cell motility and cell proliferation in a circular barrier assay," *J. R. Soc. Interface* **10**, 20130007 (2013).
- <sup>36</sup>H. L. Glenn, J. Messner, and D. R. Meldrum, "A simple non-perturbing cell migration assay insensitive to proliferation effects," *Sci. Rep.* **6**, 31694 (2016).
- <sup>37</sup>S. Martinotti, G. Calabrese, and E. Ranzato, "Honeydew honey: Biological effects on skin cells," *Mol. Cell. Biochem.* **435**, 185–192 (2017).
- <sup>38</sup>Y. H. Bae *et al.*, "Loss of profilin-1 expression enhances breast cancer cell motility by Ena/VASP proteins," *J. Cell. Physiol.* **219**, 354–364 (2009).
- <sup>39</sup>Z. Razinia *et al.*, "Stiffness-dependent motility and proliferation uncoupled by deletion of CD44," *Sci. Rep.* **7**, 16499 (2017).
- <sup>40</sup>F. Liu *et al.*, "Feedback amplification of fibrosis through matrix stiffening and COX-2 suppression," *J. Cell Biol.* **190**, 693–706 (2010).
- <sup>41</sup>C. M. Lo, H. B. Wang, M. Dembo, and Y. L. Wang, "Cell movement is guided by the rigidity of the substrate," *Biophys. J.* **79**, 144–152 (2000).
- <sup>42</sup>R. Sunyer and X. Trepat, "Durotaxis," *Curr. Biol.* **30**, R383–R387 (2020).
- <sup>43</sup>C. D. Hartman, B. C. Isenberg, S. G. Chua, and J. Y. Wong, "Vascular smooth muscle cell durotaxis depends on extracellular matrix composition," *Proc. Natl. Acad. Sci. U. S. A.* **113**, 11190–11195 (2016).
- <sup>44</sup>J. Y. Wong, A. Velasco, P. Rajagopalan, and Q. Pham, "Directed movement of vascular smooth muscle cells on gradient-compliant hydrogels," *Langmuir* **19**, 1908–1913 (2003).
- <sup>45</sup>J. R. Tse and A. J. Engler, "Stiffness gradients mimicking in vivo tissue variation regulate mesenchymal stem cell fate," *PLoS One* **6**, e15978 (2011).
- <sup>46</sup>B. C. Isenberg, P. A. Dimilla, M. Walker, S. Kim, and J. Y. Wong, "Vascular smooth muscle cell durotaxis depends on substrate stiffness gradient strength," *Biophys. J.* **97**, 1313–1322 (2009).
- <sup>47</sup>R. Sunyer *et al.*, "Collective cell durotaxis emerges from long-range intercellular force transmission," *Science* **353**, 1157–1161 (2016).
- <sup>48</sup>D. E. Discher, P. Janmey, and Y. L. Wang, "Tissue cells feel and respond to the stiffness of their substrate," *Science* **310**, 1139–1143 (2005).
- <sup>49</sup>E. A. Klein *et al.*, "Cell-cycle control by physiological matrix elasticity and in vivo tissue stiffening," *Curr. Biol.* **19**, 1511–1518 (2009).
- <sup>50</sup>G. W. McLean *et al.*, "The role of focal-adhesion kinase in cancer—A new therapeutic opportunity," *Nat. Rev. Cancer* **5**, 505–515 (2005).
- <sup>51</sup>C. T. Mierke *et al.*, "Focal adhesion kinase activity is required for actomyosin contractility-based invasion of cells into dense 3D matrices," *Sci. Rep.* **7**, 42780 (2017).
- <sup>52</sup>D. J. Webb, J. T. Parsons, and A. F. Horwitz, "Adhesion assembly, disassembly and turnover in migrating cells—Over and over and over again," *Nat. Cell Biol.* **4**, E97–E100 (2002).
- <sup>53</sup>E. D. Aguilar-Solis, I. Lee-Rivera, A. Álvarez-Arce, E. López, and A. M. López-Colomé, "FAK phosphorylation plays a central role in thrombin-induced RPE cell migration," *Cell. Signal.* **36**, 56–66 (2017).
- <sup>54</sup>D. J. Sieg, C. R. Hauck, and D. D. Schlaepfer, "Required role of focal adhesion kinase (FAK) for integrin-stimulated cell migration," *J. Cell Sci.* **112**(Pt 16), 2677–2691 (1999).
- <sup>55</sup>J. D. Owen, P. J. Ruest, D. W. Fry, and S. K. Hanks, "Induced focal adhesion kinase (FAK) expression in FAK-null cells enhances cell spreading and migration requiring both auto- and activation loop phosphorylation sites and inhibits adhesion-dependent tyrosine phosphorylation of Pyk2," *Mol. Cell. Biol.* **19**, 4806–4818 (1999).
- <sup>56</sup>Y. H. Bae *et al.*, "A FAK-Cas-Rac-lamellipodin signaling module transduces extracellular matrix stiffness into mechanosensitive cell cycling," *Sci. Signal.* **7**, ra57 (2014).
- <sup>57</sup>D. B. Rivadeneira *et al.*, "Survivin promotes oxidative phosphorylation, subcellular mitochondrial repositioning, and tumor cell invasion," *Sci. Signal.* **8**, ra80 (2015).
- <sup>58</sup>X. Li, X. Zhang, X. Li, F. Ding, and J. Ding, "The role of survivin in podocyte injury induced by puromycin aminonucleoside," *Int. J. Mol. Sci.* **15**, 6657–6673 (2014).
- <sup>59</sup>S. Lee and S. Kumar, "Actomyosin stress fiber mechanosensing in 2D and 3D," *F1000Research* **5**, 2261 (2016).
- <sup>60</sup>C. L. Hyder *et al.*, "Nestin regulates prostate cancer cell invasion by influencing the localisation and functions of FAK and integrins," *J. Cell Sci.* **127**, 2161–2173 (2014).
- <sup>61</sup>M. Prager-Khoutorsky *et al.*, "Fibroblast polarization is a matrix-rigidity-dependent process controlled by focal adhesion mechanosensing," *Nat. Cell Biol.* **13**, 1457–1465 (2011).
- <sup>62</sup>M. Vicente-Manzanares and A. R. Horwitz, "Cell migration: An overview," *Methods Mol. Biol.* **769**, 1–24 (2011).
- <sup>63</sup>C. De Pascalis and S. Etienne-Manneville, "Single and collective cell migration: The mechanics of adhesions," *Mol. Biol. Cell* **28**, 1833–1846 (2017).
- <sup>64</sup>A. P. Rickel, H. J. Sanyour, N. A. Leyda, and Z. Hong, "Extracellular matrix proteins and substrate stiffness synergistically regulate vascular smooth muscle cell migration and cortical cytoskeleton organization," *ACS Appl. Bio Mater.* **3**, 2360–2369 (2020).
- <sup>65</sup>K. R. Ammann, K. J. DeCook, M. Li, and M. J. Slepian, "Migration versus proliferation as contributor to in vitro wound healing of vascular endothelial and smooth muscle cells," *Exp. Cell Res.* **376**, 58–66 (2019).
- <sup>66</sup>H. Tahir, I. Niculescu, C. Bona-Casas, R. M. Merks, and A. G. Hoekstra, "An in silico study on the role of smooth muscle cell migration in neointimal formation after coronary stenting," *J. R. Soc. Interface* **12**, 20150358 (2015).
- <sup>67</sup>W. Shih and S. Yamada, "N-cadherin as a key regulator of collective cell migration in a 3D environment," *Cell Adhes. Migr.* **6**, 513–517 (2012).
- <sup>68</sup>C. A. Lyon, E. Koutsouki, C. M. Aguilera, O. W. Blaschuk, and S. J. George, "Inhibition of N-cadherin retards smooth muscle cell migration and intimal thickening via induction of apoptosis," *J. Vasc. Surg.* **52**, 1301–1309 (2010).
- <sup>69</sup>S. S. Rensen, P. A. Doevedans, and G. J. van Eys, "Regulation and characteristics of vascular smooth muscle cell phenotypic diversity," *Netherlands Heart J.* **15**, 100–108 (2007).



- <sup>70</sup>S. F. Louis and P. Zahradka, "Vascular smooth muscle cell motility: From migration to invasion," *Exp. Clin. Cardiol.* **15**, e75–e85 (2010).
- <sup>71</sup>J. T. Parsons, A. R. Horwitz, and M. A. Schwartz, "Cell adhesion: Integrating cytoskeletal dynamics and cellular tension," *Nat. Rev. Mol. Cell Biol.* **11**, 633–643 (2010).
- <sup>72</sup>R. S. Fischer *et al.*, "Contractility, focal adhesion orientation, and stress fiber orientation drive cancer cell polarity and migration along wavy ECM substrates," *Proc. Natl. Acad. Sci. U. S. A.* **118**, e2021135118 (2021).
- <sup>73</sup>S. Tojkander, G. Gateva, and P. Lappalainen, "Actin stress fibers—Assembly, dynamics and biological roles," *J. Cell Sci.* **125**, 1855–1864 (2012).
- <sup>74</sup>S. Sharma *et al.*, "Survivin inhibition ameliorates liver fibrosis by inducing hepatic stellate cell senescence and depleting hepatic macrophage population," *J. Cell Commun. Signal.* **18**, e12015 (2024).
- <sup>75</sup>M. Bloksgaard, M. Lindsey, and L. A. Martinez-Lemus, "Extracellular matrix in cardiovascular pathophysiology," *Am. J. Physiol. Heart Circ. Physiol.* **315**, H1687–H1690 (2018).
- <sup>76</sup>E. F. Rocnik, B. M. Chan, and J. G. Pickering, "Evidence for a role of collagen synthesis in arterial smooth muscle cell migration," *J. Clin. Invest.* **101**, 1889–1898 (1998).
- <sup>77</sup>J. Roy, M. Kazi, U. Hedin, and J. Thyberg, "Phenotypic modulation of arterial smooth muscle cells is associated with prolonged activation of ERK1/2," *Differentiation* **67**, 50–58 (2001).
- <sup>78</sup>J. Thyberg, K. Blomgren, J. Roy, P. K. Tran, and U. Hedin, "Phenotypic modulation of smooth muscle cells after arterial injury is associated with changes in the distribution of laminin and fibronectin," *J. Histochem. Cytochem.* **45**, 837–846 (1997).
- <sup>79</sup>C. Rodríguez *et al.*, "Regulation of lysyl oxidase in vascular cells: Lysyl oxidase as a new player in cardiovascular diseases," *Cardiovasc. Res.* **79**, 7–13 (2008).
- <sup>80</sup>Z. Li *et al.*, "Cyclin D1 regulates cellular migration through the inhibition of thrombospondin 1 and ROCK signaling," *Mol. Cell. Biol.* **26**, 4240–4256 (2006).
- <sup>81</sup>P. Neumeister *et al.*, "Cyclin D1 governs adhesion and motility of macrophages," *Mol. Biol. Cell.* **14**, 2005–2015 (2003).
- <sup>82</sup>Z. Zhong *et al.*, "Cyclin D1/cyclin-dependent kinase 4 interacts with filamin A and affects the migration and invasion potential of breast cancer cells," *Cancer Res.* **70**, 2105–2114 (2010).
- <sup>83</sup>Y. Zheng *et al.*, "Deficiency of filamin A in smooth muscle cells protects against hypoxia-mediated pulmonary hypertension in mice," *Int. J. Mol. Med.* **51**, 1–13 (2023).
- <sup>84</sup>E. A. Klein, Y. Yung, P. Castagnino, D. Kothapalli, and R. K. Assoian, "Cell adhesion, cellular tension, and cell cycle control," *Methods Enzymol.* **426**, 155–175 (2007).
- <sup>85</sup>A. Cretu, P. Castagnino, and R. Assoian, "Studying the effects of matrix stiffness on cellular function using acrylamide-based hydrogels," *J. Vis. Exp.* **42**, 2089 (2010).
- <sup>86</sup>J. A. Brazzo *et al.*, "Mechanosensitive expression of lamellipodin promotes intracellular stiffness, cyclin expression and cell proliferation," *J. Cell Sci.* **134**, jcs257709 (2021).